

## Feedback Active Noise Control in a Crew Rest Compartment Mock-Up

Delf Sachau<sup>1</sup>

**Abstract:** In the process of creating more fuel efficient aircraft, lightweight materials have found a broad spectrum of applications, especially in the design of aircraft cabin structures. However, in many cases considerations towards acoustic design specifications and work environment regulations require that the previously lightweight structures are treated with heavy and often bulky damping material. In some cases, as with the small rest areas of a crew rest compartment (CRC), this makes the use of active control systems attractive. In this study, the design and application of local active noise control methods in small aircraft cabin areas such as the CRC of a long range jet is discussed. The approach comprises an adaptive multichannel feedback controller with a type of virtual microphone which is implemented and tested in an acoustic mock-up. Significant noise attenuation is achieved for frequencies below 400 Hz in a zone of quiet that extends over the sides of an artificial head. Further system improvement strategies and enhancements are described such as convergence improvement by a prediction-error-filter based equalization of secondary path characteristics as well as the use of the filtered-error feedback filtered-reference LMS algorithm.

**Keywords:** Active noise control, feedback control, broadband, virtual sensing, aircraft.

### 1 Introduction

Active noise control (ANC) concepts for passenger aircraft have been developed to increase the cabin comfort of the passengers; seldom focusing on the work environment of the board crew apart from active headsets for pilots [Johansson(1999)] [Borchers, Emborg(1997)]. This is however becoming a greater concern in aircraft development due to safety regulations. It is well known that active noise control

---

<sup>1</sup> Department of Mechatronics, Helmut-Schmidt-University / University of the Federal Armed Forces, Holstenhofweg 85, 22043 Hamburg, Germany.  
Email:sachau@hsu-hh.de

can meet such requirements for frequencies below 500 Hz, offering an alternative to relatively heavy and bulky passive damping methods.

Long range jet aircraft are equipped with crew rest compartments (CRCs), which consist of multiple bunks often located in noisy sections of the aircraft, in the direct vicinity of the fuselage. The sound field in the bunk is created by multiple uncorrelated sources such as boundary layer noise and turbine-induced jet noise as well as the air conditioning, resulting in a broadband cabin disturbance. In this paper we assess the feasibility of an active control method in such a bunk for low frequency components. As opposed to propeller aircraft, where a well correlated reference signal for feedforward control is accessible by monitoring the engines, the search for a suitable reference signal in jet aircraft would, if at all possible, require high amounts of measurement devices and appropriate algorithms for reference signal synthesis. In dependence on the systems dimensions and the sensor positions, the synthesized reference would furthermore have to be calculated in such a period of time, that the feedforward control principle remains applicable. Therefore, the focus of this study is set upon the possibility of broadband feedback control.

In previous work, the concept of the active noise curtain [Sachau, Pabst (2009)] with a feedback controller arrangement was seen to be a feasible approach to global broadband control, if the path of noise-entry into the control environment is known. Here, we consider the case that the noise-entry path is unknown. Consequently, the goal of the feedback control concept is to create local zones of quiet, e.g. in the vicinity of a resting person's head, as has been done with active headrests [Tseng, Rafaely, Elliott (2002)][Pawelczyk (2003)]. Since one of the most critical parameters of feedback control is delay, especially for non-tonal noise, such systems consist of closely placed actuators and sensors that create very restricted zones of quiet and must allow for installation of the components in close proximity to the desired area of control [Elliot (2011)]. However, in a realistic application, the control equipment should be shifted out of the direct vicinity of the resting person's head which leads to the use of an enhanced feedback control method with a virtual microphone technique.

In standard controllers there is no limitation in the control frequency range as a consequence control algorithms are also applied to frequencies higher than 500Hz. Moreover, there are applications in which only a certain frequency range of the disturbance is to be controlled. As a consequence, a selection of the control frequency band is of interest. For these reasons this paper is focused on a band selective feedback single channel ANC system where the reference signal is calculated internally. The band selection is usually done with analog filters. These bandpass filters introduce delay in the system, which is critical in feedback structures. As a consequence, the selection should be performed with techniques that introduce no additional de-

lay in the signal path. Therefore the filtered-error LMS is used [Kuo, Morgan (1995)].

## 2 Experimental Setup

Figure 5b shows the mock-up of a bunk from a cabin crew rest compartment. It has a length of 2 m and 0.7 m width with an asymmetric cross-section of 0.7 m and 0.6 m height. The bottom, left and rear walls are made from 19 mm thick lumber-core plywood and can be considered to be sound hard boundaries. Top and side walls are made of 2 mm plywood panels that enable a vibro-acoustic coupling of the inner volume to the surrounding laboratory. The front, which is typically closed by a curtain, is left open. A resting person is expected to lie with his feet towards the opening. The virtual microphone is placed at the ear position of an artificial head at the closed end of the mock-up. The co-local control microphone and loudspeaker are placed 15 cm to the side of the artificial head. The mock-up itself is placed in a laboratory of 18 m length, 9 m width and 3.5 m height. Two uncorrelated sound sources are placed in the surrounding laboratory creating a disturbance in the frequency range  $100 \text{ Hz} < f < 300 \text{ Hz}$  with a total sound pressure level of 92 dB. Using the mock-up from Figure 5b, including foam damping material, the control components are placed on both sides of an artificial head as shown in Figure 1. The rapid control prototyping platform dSPACE 1006 with fast converters (dSPACE models 2004 ADC and 2102 DAC) is used for the experiments.

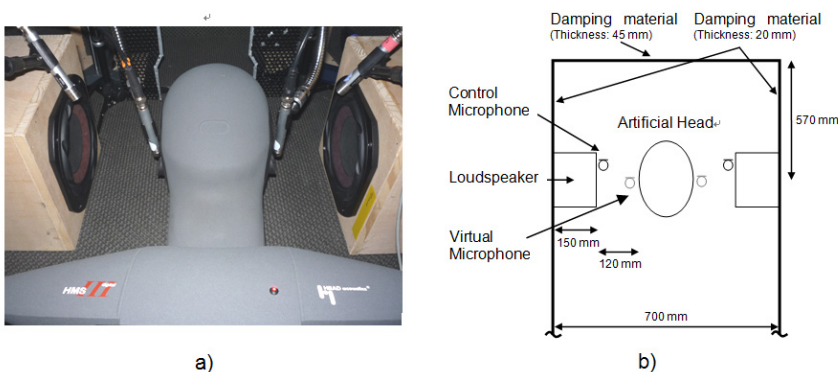


Figure 1: Multi-channel system setup.

### 3 Local Feedback Control with Virtual Microphones

#### 3.1 Secondary Paths

The filtered reference LMS algorithm (FxLMS) has a model of the secondary path located in front of the adaptive filter to compensate the effects of the secondary path. These models contain information about the impulse response of the system including the A/D and D/A converters, antialiasing and reconstruction filters, secondary loudspeaker, amplifiers and the acoustic path  $S(S_v)$  between loudspeaker and error (virtual) microphone, as shown in Figure 2. These transfer paths are measured in the mock-up with an adaptive identification procedure based on the LMS algorithm running on the control hardware. The transfer paths  $S$  and  $S_v$  are modeled with FIR filters with 512 coefficients at a sampling rate of 8 kHz using band-limited white noise ( $f < 3.2$  kHz).

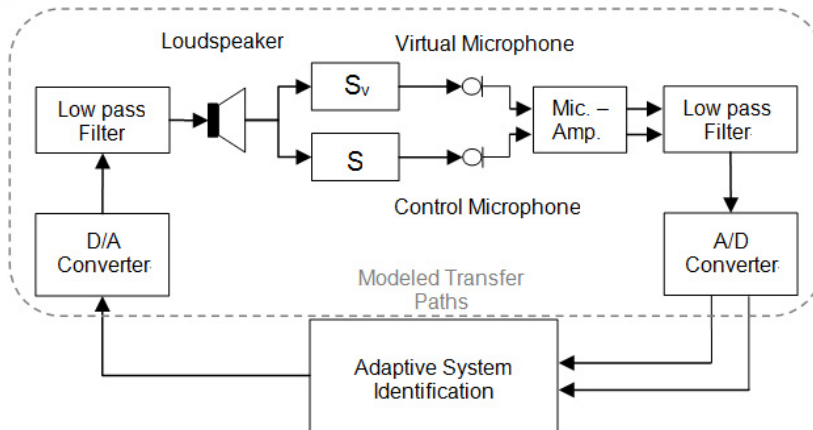


Figure 2: Transfer path modeling.

The measured paths contain especially information on the delay caused by analog filters and the acoustic paths. This dead time becomes visible in the first coefficients of the filters shown in Figure 3. Due to greater distance to the virtual microphone,  $S_v$  shows higher damping and a larger dead time. Second order Bessel filters with only  $\sim 125 \mu\text{s}$  latency are used for reconstruction and anti-aliasing. These filters with low filter slope can be used in a laboratory environment since the source of disturbance itself can be band-limited.

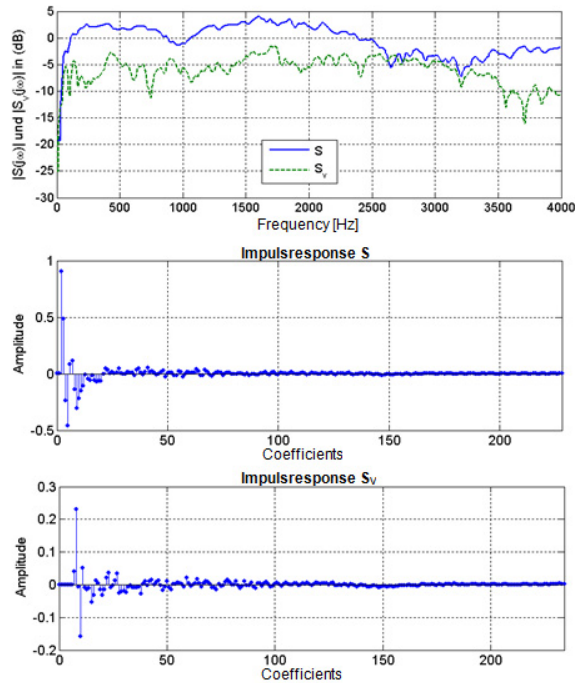


Figure 3: Magnitude spectrum and impulse responses of transfer paths  $S$  and  $S_V$ .

### 3.2 Single Channel adaptive Feedback Control

A feedback controller with the virtual microphone technique as proposed in [Pawelczyk (2003)] is used here. It is defined by a tuning stage and a control stage. In the single channel setup, the system consists of a co-local loudspeaker-microphone pair and a further microphone which is placed in the desired position of the zone of quiet at a distance from the actuator-sensor pair. The latter so called virtual microphone is only required in the tuning stage.

Following the division of the control procedure into two stages, the general principal may also be explained in two steps. First, the sound pressure at the virtual microphone is minimized to the possible extent given by the system setup. At the same time the signal behavior at the co-local so called control microphone is stored. Then the virtual microphone is removed and the loudspeaker is driven in such a manner that the previously detected state at the control microphone is reproduced. The sound pressure minimum at the previous location of the virtual microphone is thereby also reproduced, assuming that the disturbance and the transfer paths have not changed.

This principal is now applied to the feedback filtered-reference least mean squares algorithm (FBFxLMS) with internal model. The reference signal  $x'(n)$  for the FxLMS algorithm is derived through an internal model of the transfer path  $S$  to the control microphone. From Figure 4 it can be seen that during the tuning stage the controller minimizes the error signal  $e_v(n)$  of the virtual microphone. At the same time, coefficients of the filter  $H(z)$  are adapted in order to minimize  $e'(n)$ , the difference of the control microphone signal  $e_c(n)$  and the filter output  $e_H(n)$ . Therefore, filter  $H(z)$  contains information on the error signal  $e_c(n)$  when  $e_v(n)$  is minimal. Under the assumption of optimal reference signal synthesis and stationary acoustic disturbances, it is the transfer function between the disturbance at the control microphone  $d_c(n)$  and the signal at the control microphone during the tuning stage.

In the control stage  $H(z)$  is no longer adaptive, see red and black lines in Figure 4. The algorithm minimizes  $e'(n)$ , thereby setting the pressure signal at the control microphone to its previous state which in turn recreates the zone of quiet at the position of the virtual microphone under the given assumptions.

As the results in terms of spectral shape and zone of quiet are similar to the multi-channel case, they are shown in the following section.

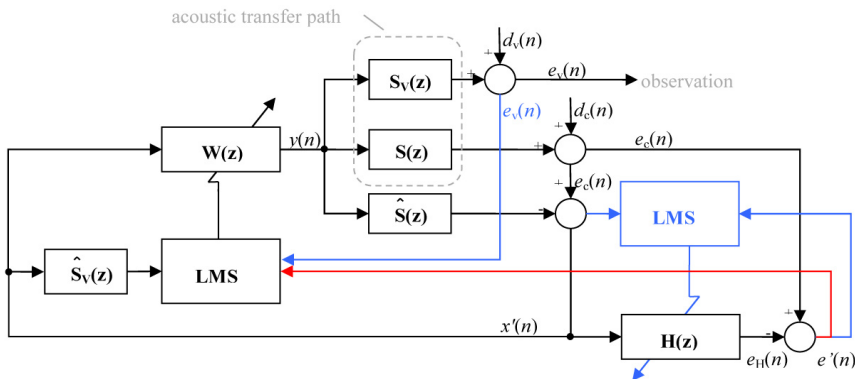


Figure 4: Tuning and control stage of a single channel FBFxLMS with virtual microphone.

### 3.3 Multi-Channel Feedback Control

Having demonstrated the controller's capability in a single channel setup, considerations are now taken towards a multiple channel implementation with 2 loudspeakers and co-local control microphones as well as 2 virtual microphones in order to create zones of quiet at both sides of a resting person's head.

The multichannel controller, as described in [Pawelczyk (2003)], is implemented with 300 coefficients for path modeling, 600 coefficients for filter  $H(z)$  and 800 coefficients for the control filters. The system sampling rate is set to 8 kHz. The virtual microphones are left in their respective positions during the control stage for observation purposes. With this system setup a broadband noise reduction of approx. 20 dB is achieved at both ears of the artificial head. As the spectral shape is similar on both sides of the artificial head, only the spectrum at the virtual microphone at the right ear is shown in Figure 5a.

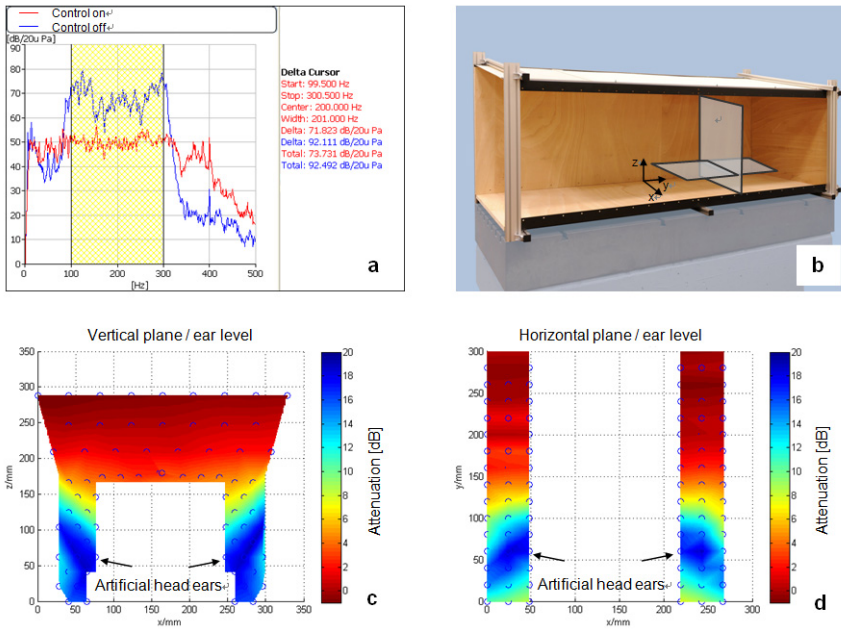


Figure 5: Multi-channel control. (a) spectrum at right virtual microphone, (b) mapping planes, (c) vertical mapping, (d) horizontal mapping

The controlled sound field is mapped with a vertical microphone array which is moved in steps of 2 cm along the cabin. The 72 microphone positions are marked as circles in Figure 5c. As shown, the microphones are distributed evenly in 2 zones of the vertical plane. In the area on the sides of the head microphone spacing is 2 cm. Above the head, the spacing is 4 cm. Figure 5c,d show the linearly interpolated results of the mapping in the horizontal and vertical planes at ear-level as shown in Figure 5b. The zone of quiet with at least 10 dB attenuation is centered at the virtual microphone which leads to an area of approximately 120 mm in height and width around a resting person's ears. The attenuation quickly drops by more than

10 dB within a few centimeters in the transition zone at the upper side of the head. The SPL is not significantly increased in the vicinity of the artificial head outside of the area of control.

#### 4 Bandlimitation by the Filtered Error Algorithm

In the previous chapter the disturbance is limited to a frequency range. With the method proposed in this chapter a frequency band of a broader disturbance can be controlled with the same level of attenuation [Elliot (2011)]. The achieved attenuation is dependent on the bandwidth of the disturbance, being smaller with broader disturbances. The standard feedback controller performs cancellation with no frequency range limitation. Therefore, the antialiasing and reconstruction filters have the additional function to limit the control bandwidth. Since one of the main features in the structure analyzed here is the possibility to control a specific frequency band, which will be explained in following sections, this extra purpose of the antialiasing and reconstruction filters is not needed. These filters can be changed to filters with a higher corner frequency resulting in lower delay.

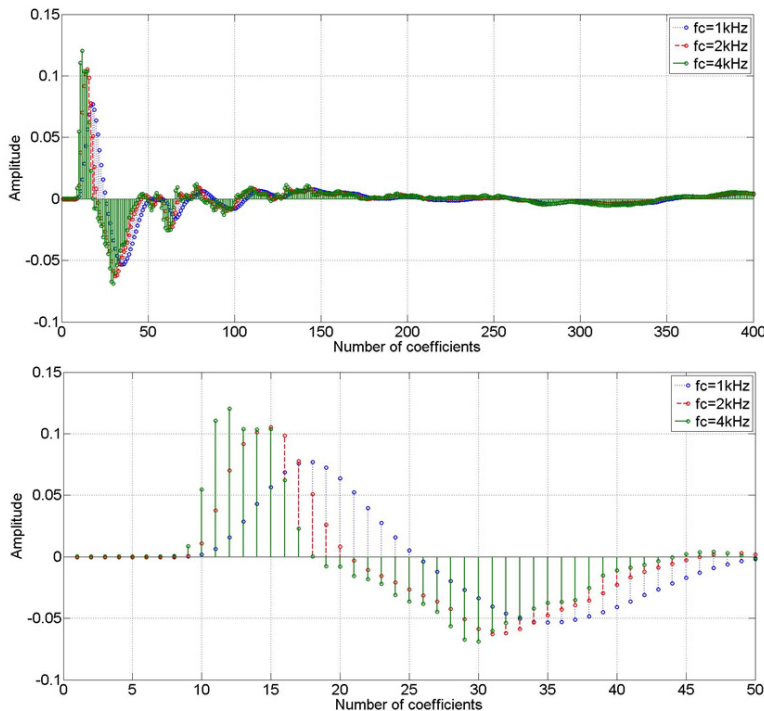


Figure 6: Impulse responses of secondary path with three different configurations.



The impulse responses of the secondary path model with different corner frequencies in the antialiasing filters are shown in Figure 6. The secondary path is modeled with the LMS adaptive identification using 400 coefficients and 16 kHz sampling frequency. Antialiasing and reconstruction filters are second order Bessel filters. As shown in Figure 6 there is a reduction in dead time using filters with higher corner frequency  $f_c$ . The dead time and averaged group delay without null samples within the control band are shown in Table 1 for three configurations of antialiasing and reconstruction filters.

Table 1:

Corner frequency	1kHz	2kHz	4kHz
Dead time ( $\mu\text{sec}$ )	625	562.5	500
Averaged group delay ( $\mu\text{sec}$ )	656.25	506.25	443.75
Total ( $\mu\text{sec}$ )	1281.25	1068.75	943.75

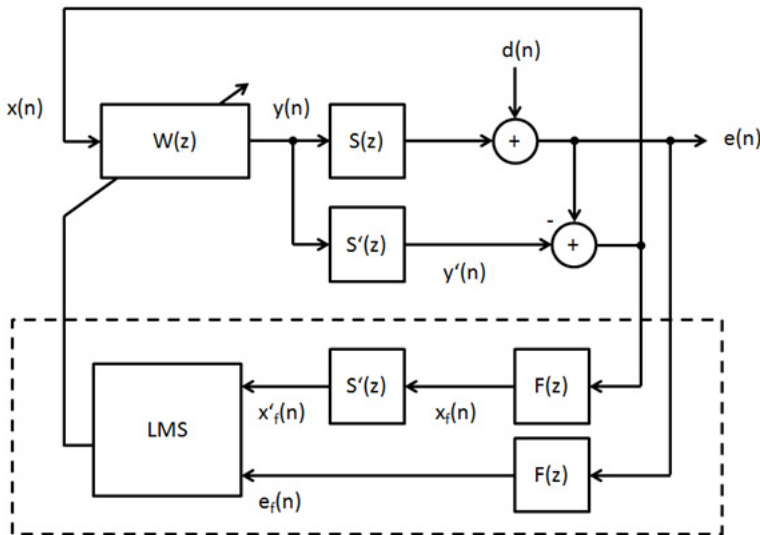


Figure 7: Block diagram of the FE-FBFxLMS algorithm.

#### 4.1 The Algorithm

The FE-FBFxLMS algorithm selects the frequency range under control without additional delay, [De Dios, Pabst, Sachau(2012)]. Figure 7 shows the block diagram. The error signal  $e(n)$  and thereby the reference  $x(n)$  is bandpass filtered in the auxiliary loop by  $F(z)$  which is the main difference in the standard implementation of the feedback filtered-X LMS (FBFxLMS). The weights of the adaptive filter  $W(z)$  are updated by  $w(n+1) = w(n) - \mu e_f(n)[x_f(n) * s'(n)]$  with the *filtered* error  $e_f(n)$ , the *filtered* reference  $x_f(n)$  and the secondary path model  $S'(n)$ . Because the weights are adapted by the filtered signals, the adaptive filter in the main loop acts as a bandpass filter. As a consequence, the level of attenuation is only dependent on the selected bandwidth and not on the disturbance bandwidth. A minor drawback of the FE-FBFxLMS is a slower convergence rate of the adaptive filter because in relation to the reference the filtered signals are delayed.

#### 4.2 Experimental Results

The tests are performed using a single channel structure. A primary noise source is placed in the laboratory creating a disturbance with 800 Hz bandwidth. The error microphone is placed 12cm away from the secondary loudspeaker.

The standard and the filtered-error feedback FxLMS are compared. Both systems are working with 16 kHz sampling frequency and different corner frequencies are set in the FE-FBFxLMS controller. In Figure 8a the standard FBFxLMS is used to control the disturbance. In this setup the corner frequency of antialiasing and reconstruction filters is set to 1 kHz. This standard controller tries to cancel the whole frequency range of the disturbance. Attenuation of 4 dB is achieved. Focusing on a specific band (200-300Hz), attenuation up to 5 dB is reached.

The same disturbance with the same antialiasing and reconstruction filter configuration is controlled with the FE-FBFxLMS. The bandpass filter has corner frequencies of 200 Hz and 300 Hz. The attenuation achieved in the selected band is 14 dB, see Figure 8b.

Using the analyzed structure, higher attenuation is achieved in the specified band. A slight amplification of around 2-3 dB is obtained in the whole frequency range. With this structure a reduction of the delay introduced with the secondary path modeling, as mentioned in previous sections, can be performed using different configurations of antialiasing filters. The same disturbance is controlled with the FE-FBFxLMS controller but using a higher corner frequency of 4 kHz in the antialiasing and reconstruction filters. Figure 8c shows that an attenuation of 17dB is achieved in the selected band.

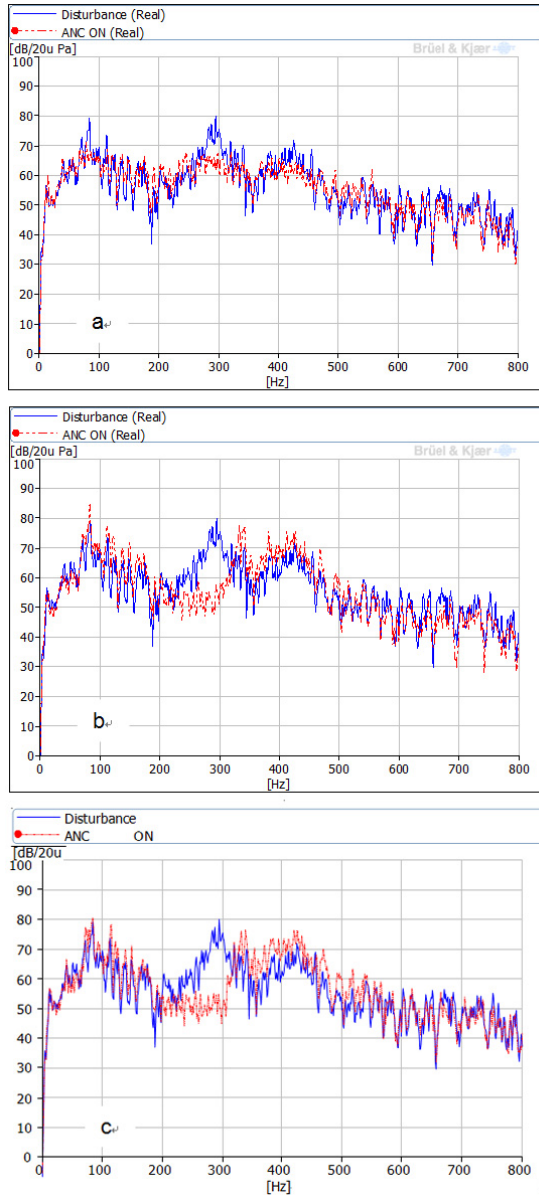


Figure 8: Disturbance and controlled signal. (a) FBFxLMS,  $f_c = 1$  kHz, (b) FE-FBFxLMS,  $f_c = 1$  kHz, (c) FE-FBFxLMS,  $f_c = 4$  kHz

## 5 Conclusions

The general feasibility of a feedback approach to a broadband active noise problem in a crew rest compartment cell with multiple uncorrelated noise sources has been

shown. The method of virtual microphones shifts the zone of quiet to the desired position. A multi-channel approach achieves an attenuation of 15 – 20 dB in a frequency range of 100 Hz – 300 Hz at the ears of an artificial head. The zone of quiet with at least 10 dB attenuation is large enough to cover the sides of a person's head. An increase in the acoustic transfer path length to the virtual position leads to an increase in delay, thereby limiting the actual system performance. Hence, the optimal placement of the actuators and sensors is restricted to a zone in the vicinity of the head.

The FE-FBFxLMS reduces the delay introduced in the secondary path due to analogue filters. Therefore a higher attenuation can be achieved in a chosen frequency range than with the standard FBFxLMS. This higher attenuation comes with the drawbacks of a slower convergence rate and a small amplification out of the selected frequency band.

### Acknowledgments

Funding by the City of Hamburg in the framework of LuFoHH to enable this project is gratefully acknowledged.

### References

- Johansson, S. et al.** (1999): Control Approaches for Active Noise Control of Propeller-induced Cabin Noise evaluated from Data from a Dornier 328 Aircraft, *In Proc. 6th int. Congress on Sound and Vibration*, Copenhagen, pp.1611-1618.
- Borchers, I.U.; Emborg, U. et al.** (1997): Advanced Study for Active Noise Control in Aircraft (ASANCA), *Fourth Aircraft Interior Noise Workshop*, NASA Langley Research Center, USA, pp.129-141.
- Sachau, D.; Pabst, O.** (2009): Adaptive Control of Broadband Noise in a Light Jet. *In Proc. Internoise 2009, Ottawa, Canada*.
- Tseng, W. K.; Rafaely, B.; Elliott, S.J.** (2002): Performance limits and real-time implementation of a virtual microphone active headrest, *in Proc. Active '02*, Southampton, UK, pp.1231-1242.
- Pawelczyk, M.** (2003): Adaptive Noise Control Algorithms for Active Headrest System, *Control Engineering Practice 12*, pp.1101-1112.
- Elliott, S. J.** (2011): *Signal Processing for Active Control*. Academic Press, San Diego, CA.
- Kuo, S. M.; Morgan D. R.** (1995): *Active Noise Control Systems: Algorithms and DSP Implementations*, John Wiley & Sons, NY.

**Pabst, O.; Sachau, D.** (2010): Broadband Active Noise Control in a Cabin Crew Rest Compartment, Proceedings Internoise 2010, Lisbon, Portugal, 13-16 June.

**Morgan, D.R.; Thi, J.C.** (1995): A delayless subband adaptive filter architecture, IEEE Transactions on Signal Processing, vol.43, no.8, pp.1819-1830.

**Kuo, S. M.; Tsai, J.** (1994): Residual noise shaping technique for active noise control systems, *Journal of Acoustic Society America*, vol.95, pp.1665.

**Pabst, O.** (2011): Entwurf eines Systems zur breitbandigen Lärminderung in Ruhebereichen von Flugzeugen, Dissertation, Helmut Schmidt Universität Hamburg.

**De Dios, J. A.; Pabst, O.; Sachau, D.** (2012): Feedback active noise control with a Filtered-Error Algorithm. Proceedings 19<sup>th</sup> International Congress on Sound and Vibration, Vilnius, Lithuania.

